JACS
JOURNAL OF THE AMERICAN CHEMICAL SOCIETY
pubs.acs.org/JACS
Article

Hydroalkylation of Unactivated Olefins via Visible-Light-Driven Dual Hydrogen Atom Transfer Catalysis

Guangyue Lei,[§] Meichen Xu,[§] Rui Chang, Ignacio Funes-Ardoiz,* and Juntao Ye*

Cite This: *J. Am. Chem. Soc.* 2021, 143, 11251−11261
Read Online
ACCESS | Metrics & More | Article Recommendations | Supporting Information

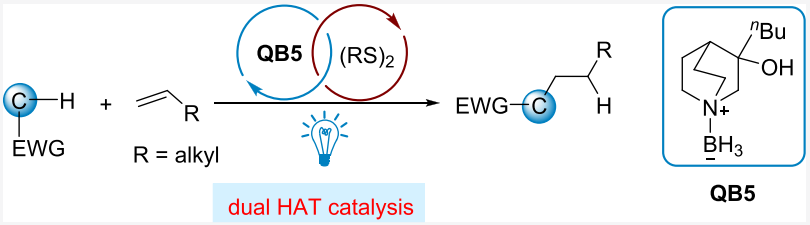

ABSTRACT: Radical hydroalkylation of olefins enabled by hydrogen atom transfer (HAT) catalysis represents a straightforward means to access C(sp^3)-rich molecules from abundant feedstock chemicals without the need for prefunctionalization. While Giese-type hydroalkylation of activated olefins initiated by HAT of hydridic carbon−hydrogen bonds is well-precedented, hydroalkylation of unactivated olefins in a similar fashion remains elusive, primarily owing to a lack of general methods to overcome the inherent polarity-mismatch in this scenario. Here, we report the use of visible-light-driven dual HAT catalysis to achieve this goal, where catalytic amounts of an amine-borane and an in situ generated thiol were utilized as the hydrogen atom abstractor and donor, respectively. The reaction is completely atom-economical and exhibits a broad scope. Experimental and computational studies support the proposed mechanism and suggest that hydrogen-bonding between the amine-borane and substrates is beneficial to improving the reaction efficiency.

INTRODUCTION

Hydrogen atom transfer (HAT) is a key elementary step in free-radical reactions and biological transformations.[1,2] With the rapid development of visible-light-mediated photocatalysis,[3,4] photoinduced H atom abstraction has evolved into a powerful strategy for building molecular complexity from readily available substrates without the need for prefunctionalization.[1] As the selectivity of HAT events is mainly governed by enthalpy and polar effects,[5,6] high levels of efficiency and regioselectivity could be achieved by fine-tuning bond dissociation energy (BDE) and philicity of the HAT catalyst. To date, most of the H atom abstracting radicals that derive from indirect HAT catalysts[7] and direct HAT catalysts such as diaryl ketones,[8] decatungstate anion,[9] eosin Y,[10] and uranyl cation,[11] have electrophilic character (Figure 1A).[1j,6b] Consequently, substrate activation via H atom abstraction is largely limited to those containing hydridic R−H (R = C, Si, B, etc.) bonds and electron-neutral aliphatic C−H bonds because of a polarity-matching effect.[6] To make electron-deficient C−H bonds amenable to H atom abstraction, nucleophilic radicals resulting from hydridic HAT reagents with appropriate bond strength are required. In this regard, Roberts' seminal electron paramagnetic resonance (EPR) studies demonstrated that nucleophilic amine- and phosphine-boryl radicals are competent for selective abstraction of electron-deficient C−H bonds.[6a] Nevertheless, synthetic reactions *catalyzed* by these ligated boranes remain rare,[12] mainly due to the challenges associated with the turnover of the borane catalyst using organic peroxides as the radical initiator.

Radical hydroalkylation of olefins represents a straightforward approach for the construction of C(sp^3)−C(sp^3) bonds from abundant feedstock chemicals.[13] Given the nucleophilic character of most carbon-centered radicals, their addition to olefins is largely limited to polarity-matched, electron-deficient olefins (Giese reaction)[13a] and styrene derivatives as their addition to unactivated olefins is often too sluggish to be synthetically useful.[14] In Giese-type reactions, following the radical addition, reduction of the radical adduct by a protic HAT catalyst then furnishes the hydroalkylation product via sequential single-electron transfer/proton transfer (SET/PT) or HAT (Figure 1B).[4i] In contrast, hydroalkylation of unactivated olefins enabled by HAT catalysis remains underexplored,[15] although protocols relying on SET reduction or oxidation of prefunctionalized radical precursors such as organic halides and diazo compounds have been documented.[16] In order to generate electrophilic alkyl radicals

Received: June 6, 2021
Published: July 16, 2021

https://doi.org/10.1021/jacs.1c05852
J. Am. Chem. Soc. 2021, 143, 11251−11261

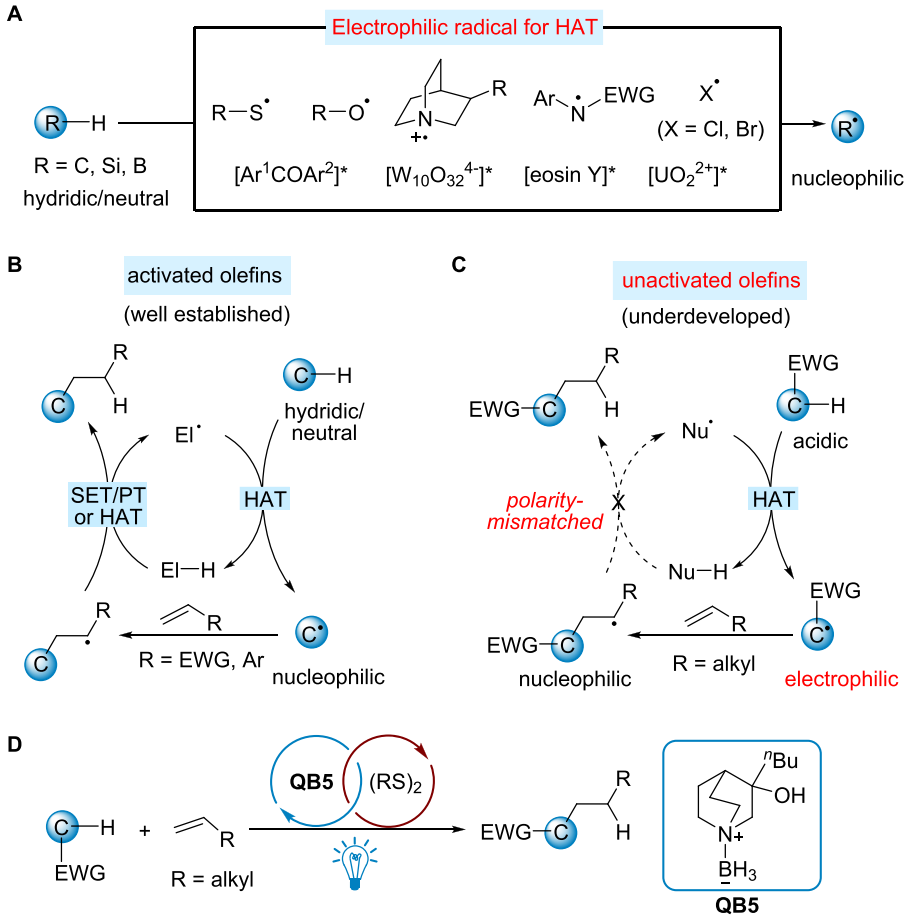

Figure 1. Strategies for hydroalkylation of activated and unactivated olefins via photoinduced hydrogen atom transfer (HAT) catalysis. (A) Commonly used HAT catalysts are mostly electrophilic and thus generate nucleophilic radicals upon HAT. (B) Well-established Giese-type hydroalkylation of activated olefins initiated by HAT of hydridic carbon–hydrogen bonds. (C) Hydroalkylation of unactivated olefins with substrates bearing electron-deficient C–H bonds using a nucleophilic HAT catalyst. (D) This work, hydroalkylation of unactivated olefins via visible-light-driven dual HAT catalysis. EWG, electron-withdrawing group; El•, electrophilic radical; Nu•, nucleophilic radical.

directly from C–H bonds, a hydridic HAT catalyst that can easily form a nucleophilic H atom abstracting radical is required (Figure 1C). However, the terminating HAT event between the nucleophilic radical adduct and the hydridic HAT reagent is polarity-mismatched. This renders oxidation of the radical adduct to a carbocation more favorable due to the low oxidation potential of the alkyl radical [$E_{1/2}^{ox}$ = 0.47 V versus saturated calomel electrode (SCE) in MeCN for 2-propyl radical],[17] which typically leads to vicinal difunctionalized products[18] or substituted olefins.[19] To overcome this fundamental limitation, we questioned whether a dual HAT catalysis strategy, that is, a combination of a hydridic and a protic HAT catalyst, could circumvent the problem. In particular, we hypothesized that synergistic action of a ligated borane[6a,20] and a thiol could potentially enable atom-economical radical hydroalkylation of unactivated olefins with substrates bearing electron-deficient C–H bonds, thereby avoiding the use of prefunctionalized radical precursors (Figure 1D). Herein, we report the successful execution of this design plan.

RESULTS AND DISCUSSION

Reaction Development. At the outset of our investigation, we recognized that identification of a ligated borane that can generate nucleophilic boryl radical under photoredox catalysis is the key to this dual HAT strategy. Given that recent studies have demonstrated that *N*-heterocycle carbene (NHC)-boryl radicals could easily be generated from NHC-boranes under photoinduced HAT or single-electron oxidation,[20,21] we initiated our study by evaluating NHC-borane complex **NHC-BH$_3$** as the hydridic HAT catalyst using various thiols (not shown) as the protic HAT catalyst for the reaction of 4-phenyl-1-butene **1** and dimethyl malonate **2** (Table 1). Unfortunately, only thiol–ene reaction[22] byproducts were formed in most cases without any detectable desired product, presumably due to the relative low BDE of the B–H bond (70–80 kcal/mol)[23] as compared to the acidic C–H bond of **2** (BDE = 93 kcal/mol).[24] Gratifyingly, when quinuclidine-borane **QB1**, which has a much stronger B–H bond (BDE = 100 kcal/mol, see Figure 5A) and was utilized by Roberts as H atom abstractor under high-energy UV irradiation using peroxides as initiators,[12] was tested in the presence of 2,4,6-triisopropylbenzenethiol (TRIPSH), the desired hydroalkylation product **3** was obtained in 45% yield using [Ir(dF(CH$_3$)-ppy)$_2$(dtbbpy)]BAr$^F_4$ (**PC**) as the photocatalyst (entry 2), with the rest of the mass balance being unreacted starting materials. Inspired by recent advances in hydrogen bond-assisted photoinduced radical reactions,[1c,25] we envisioned that introduction of a hydrogen bond donor in the amine-borane complex might accelerate the desired HAT due to hydrogen

https://doi.org/10.1021/jacs.1c05852
J. Am. Chem. Soc. 2021, 143, 11251–11261

Table 1. Reaction Optimization[a]

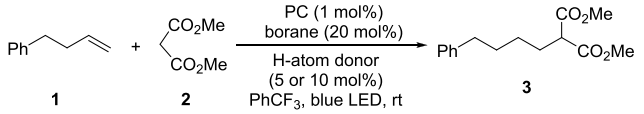

entry	borane	H atom donor	yield (%)[b]
1	**NHC-BH$_3$**	TRIPSH	0
2	**QB1**	TRIPSH	45
3	**QB2**	TRIPSH	75
4	**QB3**	TRIPSH	46
5	**QB4**	TRIPSH	45
6	**QB5**	TRIPSH	89
7	**QB5**	(TRIPS)$_2$	92 (91)[c]
8[d]	**QB5**	(TRIPS)$_2$	91
9	–	(TRIPS)$_2$	7
10	**QB5**	–	18
11	–	–	0
12[e]	**QB5**	(TRIPS)$_2$	0
13[f]	**QB5**	(TRIPS)$_2$	0

[a]Reaction conditions: All reactions were carried out with **1** (0.2 mmol), **2** (0.8 mmol), **PC** (1 mol %), borane (20 mol %), TRIPSH (10 mol %) or (TRIPS)$_2$ (5 mol %), and $PhCF_3$ (0.5 mL) unless otherwise noted. The reactions were irradiated with a 40-W Kessil blue LED under nitrogen atmosphere for 48 h. [b]Yields were determined by ^{1}H NMR analysis of the crude reaction mixture. [c]Isolated yield. [d]Benzene as the solvent. [e]Without **PC**. [f]Without light. BAr^F_4: tetrakis[3,5-bis(trifluoromethyl)-phenyl]borate.

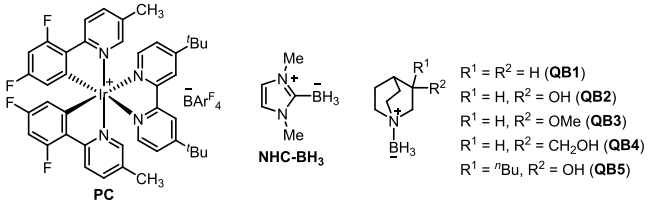

bonding interaction with the carbonyl group of the substrate. To our delight, a dramatic increase in the yield of **3** was indeed observed when readily available 3-quinuclidinol−borane **QB2** was utilized (75%, entry 3). Boranes **QB3** with the hydroxyl group protected or **QB4** derived from 3-(hydroxymethyl)-quinuclidine proved to be less effective (entries 4 and 5), indicating the hydroxyl group and its position play a pivotal role. Further evaluation of substituent effect on the quinuclidinol scaffold led to the identification of borane **QB5** as the optimal hydridic HAT catalyst and the yield of product **3** was increased to 89% (entry 6, see section 2 of the Supporting Information). Interestingly, replacing the thiol with 5 mol % of easy-to-handle and odorless bis(2,4,6-triisopropyl-phenyl) disulfide [(TRIPS)$_2$] provided **3** in 91% yield upon isolation (entry 7).[26] Same efficiency was observed when benzene was used as the solvent (entry 8). Notably, control experiments confirmed that visible light and photocatalyst are indispensable while the absence of the borane catalyst or the disulfide resulted in a significant decrease in the yield of **3** (entries 9−13).

Reaction Scope. With the optimal conditions in hand, we explored the scope and limitations of the reaction (Figure 2). A diverse array of active methylene compounds was found to be suitable alkyl radical precursors. In addition to 1,3-diesters (**4**−**6**), triethylmethanetricarboxylate (**7**), β-ketoester (**8**), β-ketoamide (**9**), carbamoylacetates with a free NH_2 (**10**), an *N*-alkyl (**11**) or an *N*-aryl (**12**) group all showed high reactivity to yield the products in 81−93% yields. Of note, nitriles such as ethyl cyanoacetate (**13**), malonitrile (**14**), and β-ketonitrile (**15**) all reacted well to give the desired products in good yields despite the fact that addition of amine-boryl radicals to nitrile groups has been documented.[27] Furthermore, no over-oxidation of radical adducts or α,α-dialkylation of the 1,3-dicarbonyl derivatives was observed under the reaction conditions, highlighting the mildness of the current protocol compared to conventional chemical oxidation conditions[28] or alkylation with alkyl halides under basic conditions. Simple carboxylic esters such as methyl propionate is not reactive under the conditions, presumably due to the difficulty in generating the corresponding weakly electrophilic carbon radical under our conditions (vide infra).

The scope of the olefin was then examined and a high level of functional group tolerance was observed. Mono- or disubstituted unactivated olefins bearing a free hydroxyl (**17**), tosylate (**18**), chloro (**19**), carboxylic ester (**20**), ketone (**21**), ether (**22**), silyl (**23**), boronate (**24**), amide (**25**), cyano (**26**, **27**), and carbamate (**28**, **29**) groups were all well tolerated, providing the desired products in 59−96% yields. Olefins with alkyl rings of various size (**30**−**33**), electron-rich carbazole (**34**), or electron-deficient arenes (**35**−**37**) all underwent the reaction smoothly. While Minisci-type borylation of pyridines was achieved using an amine-borane very recently,[29] no such reactivity was observed under our conditions, and the desired product **37** was obtained in 70% yield. Internal olefins such as *cis*-cyclooctene and 2,3-dimethyl-but-2-ene were also amenable, giving rise to the products **38** and **39** in 95% and 76% yields, respectively. As expected, the reactions of 2-methylbut-2-ene with dimethyl malonate or *N*-phenylcarbamoylacetate afforded the products **40** and **41** as mixtures of regioisomers. When 1,5-hexadiene was subjected to the reaction conditions, 1,6-dialkylated product **42** was obtained in 78% yield. To further illustrate the utility of the present method, a diverse range of structurally complex olefins derived from drug molecules, natural products, and materials precursors were examined (Figure 3). To our delight, the existing functional groups and structural complexity exerted a negligible influence on the efficiency of the reaction, leading to potentially valuable products **43**−**67** in moderate to excellent yields. The structure of product **54** was confirmed by X-ray diffraction analysis. The practicability of the methodology was further demonstrated by the synthesis of **38**, **63**, and **66** on preparative scales. Overall, the current dual HAT-enabled hydroalkylation protocol exhibits much broader substrate scope with higher functional group tolerance compared to existing oxidant- or base-promoted approaches.[28,30]

Mechanistic Investigations. Next, we turned our attention to investigate the mechanism of the reaction. The radical nature of the reaction was first confirmed by a series of experiments (Figure 4A). A radical trapping experiment with 2,2,6,6-tetramethylpiperidine-1-oxyl (TEMPO) completely shut down the reactivity with two radical adducts **68** and **69** being detected by high resolution mass spectrometry (HRMS), indicating the involvement of the electrophilic malonyl radical and the thiyl radical, respectively. Radical clock experiment using α-cyclopropyl-styrene **70** provided the ring-opened product **71** in 67% yield as a mixture of *E*/*Z* isomers. Similarly, bicyclic terpene β-pinene also afforded the ring-opened product **72** in 69% yield. Stern−Volmer luminescence quenching experiments showed that the disulfide efficiently quenches the excited state of the iridium photocatalyst while

https://doi.org/10.1021/jacs.1c05852
J. Am. Chem. Soc. 2021, 143, 11251−11261

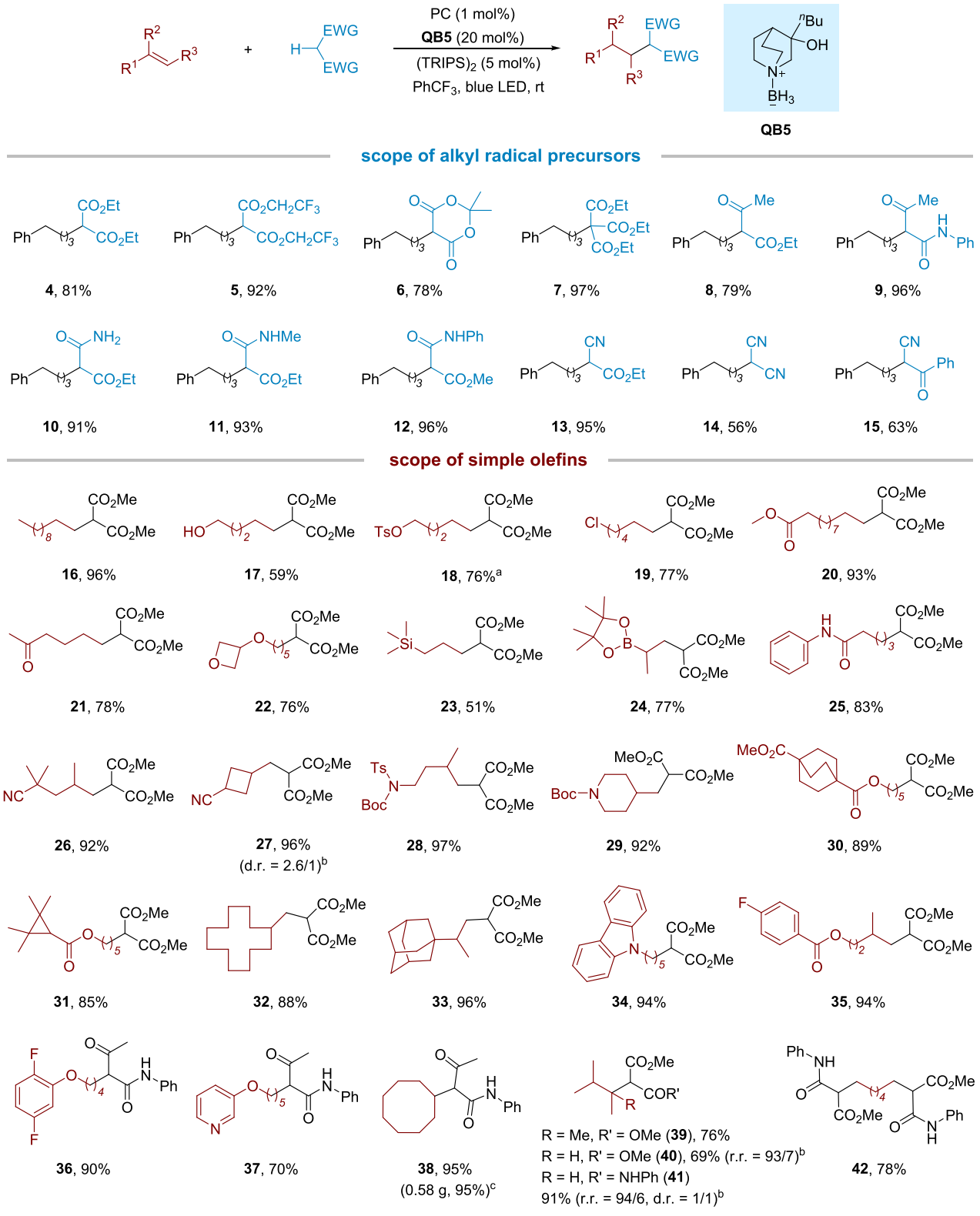

Figure 2. Hydroalkylation of unactivated olefins enabled by dual HAT catalysis. Reaction conditions: olefin (0.2 mmol), active methylene compound (0.4 or 0.8 mmol), **PC** (1 mol %), **QB5** (20 mol %), and $(TRIPS)_2$ (5 mol %) in $PhCF_3$ (0.5 mL), irradiation with a 40-W Kessil blue LED at room temperature for 48 h unless otherwise noted; Isolated yields are reported. see Supporting Information for experimental details. [a]Reaction performed with **QB5** (40 mol %). [b]Diastereomeric ratio (d.r.) and regioisomeric ratio (r.r.) were determined by ^1H NMR and GC-MS or LC-MS analysis of the crude reaction mixture. [c]Reaction performed on 2 mmol scale.

all the other components or combinations do not (Figure S13 in the SI). Given the reduction potential of $(TRIPS)_2$ ($E_{1/2}^{red}$ = −1.78 V vs SCE in MeCN),[31] SET reduction of the disulfide by the excited-state of the photocatalyst Ir(III)* ($E_{1/2}^{IV/III*}$ = −0.92 V vs SCE in MeCN)[32] is unlikely to be operative. On the basis of literature precedents,[22c,26a] we attributed the

https://doi.org/10.1021/jacs.1c05852
J. Am. Chem. Soc. 2021, 143, 11251−11261

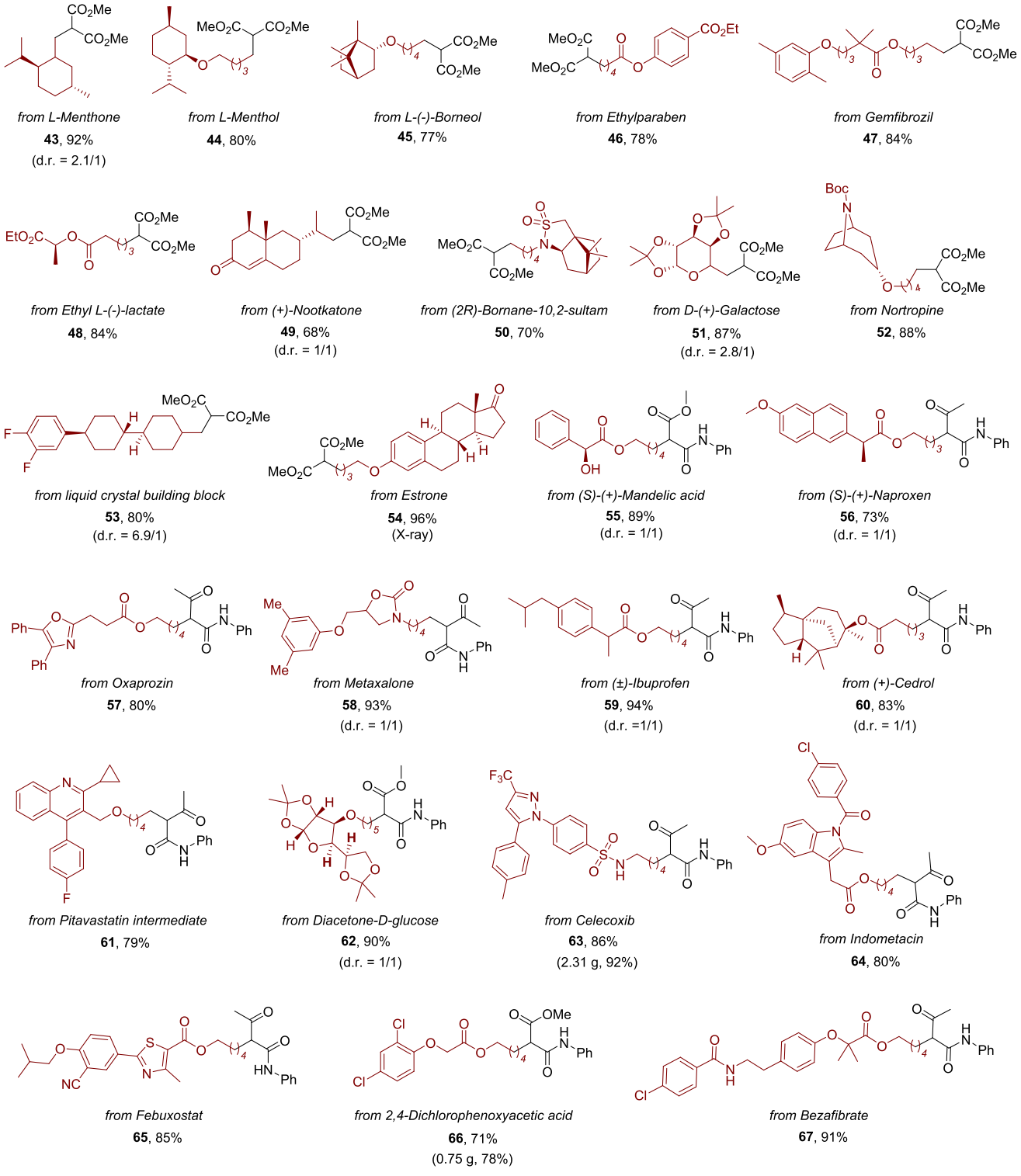

Figure 3. Hydroalkylation of complex olefins derived from natural products or drugs. See Figure 2 and SI for reaction conditions.

strong phosphorescence quenching to an energy transfer event between the Ir(III)* and the disulfide. Moreover, cyclic voltammetry studies indicate that SET oxidation of the amine-borane catalyst **QB5** ($E_{p/2}^{ox}$ = +1.27 V vs SCE in MeCN, see SI for details) by the excited-state of the photocatalyst Ir(III)* ($E_{1/2}^{III*/II}$ = +0.97 V vs SCE in MeCN)[32] is not thermodynamically favorable, suggesting a reductive quenching pathway is unlikely to be operative. Conducting light on/off experiments with alternating periods of irradiation and darkness for the reaction of **1** and **2** revealed that constant irradiation is required as no conversion was observed in the dark period (Figure S14 in the SI). Moreover, the quantum yield of the reaction between **1** and **2** was determined to be 0.32. Collectively, these results indicate that radical chain propagation, if present, is not the major pathway for the current hydroalkylation reaction.

On the basis of the above mechanistic studies, a plausible mechanism was proposed (Figure 4B). Upon blue light

https://doi.org/10.1021/jacs.1c05852
J. Am. Chem. Soc. 2021, 143, 11251−11261

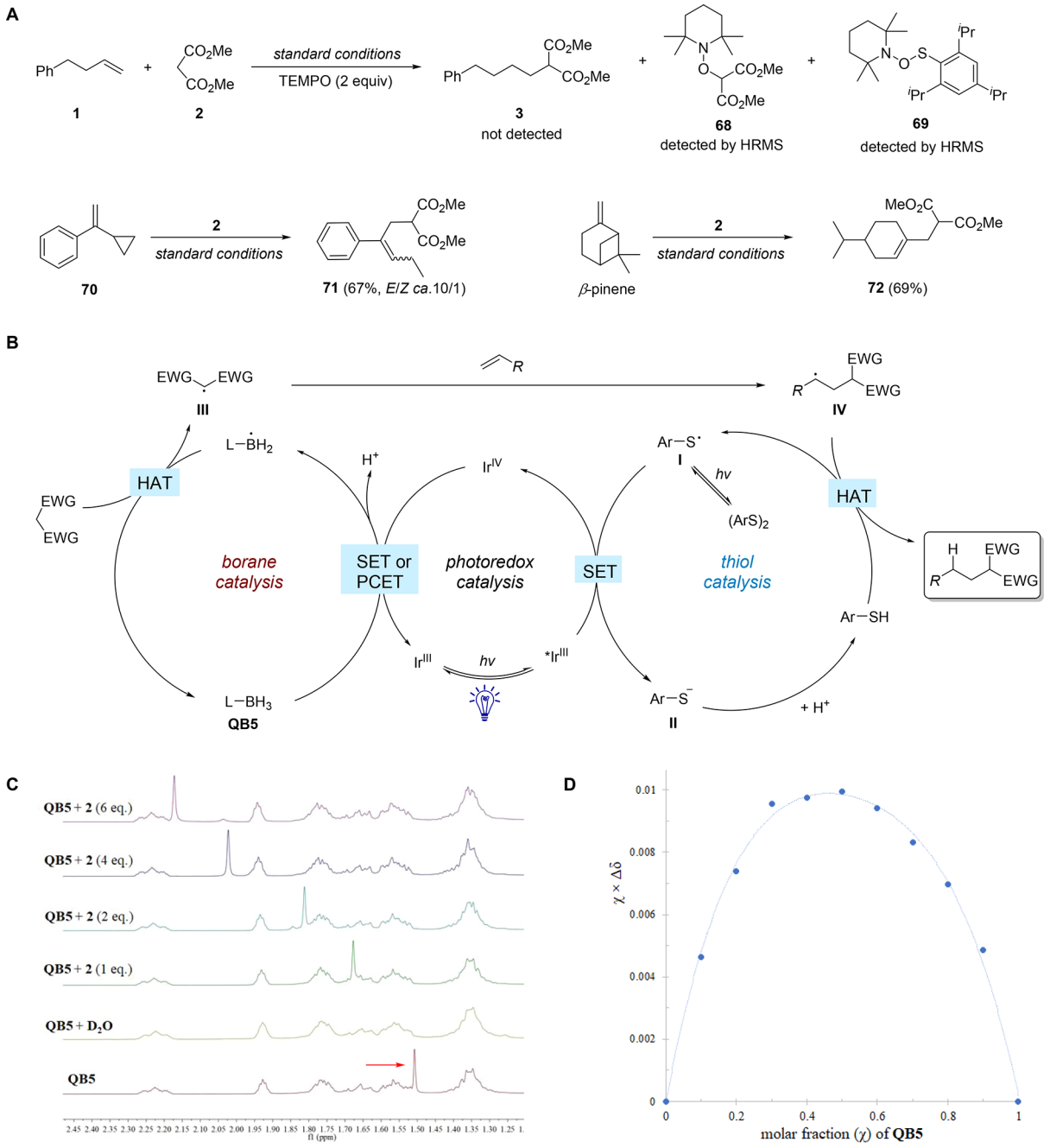

Figure 4. Mechanistic studies. (A) Radical trap and radical clock reactions. (B) Proposed reaction mechanism. (C) ^{1}H NMR titration experiments using **QB5** and dimethyl malonate **2**. The resonance signal corresponding to the hydroxyl group of **QB5** (indicated with a red arrow) is downfield shifted upon increasing concentrations of dimethyl malonate **2** (bottom to top). (D) Job plot indicates the formation of a complex between **QB5** and dimethyl malonate **2** with 1:1 stoichiometry.

irradiation, the disulfide undergoes photolytic homolysis to afford aryl thiyl radical **I**, which could be readily reduced ($E[PhS^{\bullet}/PhS^{-}]$ = 0.16 V vs SCE)[33] by the excited state of the photocatalyst Ir(III)* ($E_{1/2}^{IV/III*}$ = −0.92 V vs SCE in MeCN)[32] to provide aryl thiolate **II** and the oxidized form of the photocatalyst. The resulting strongly oxidizing Ir(IV) species ($E_{1/2}^{IV/III}$ = +1.51 V vs SCE in MeCN)[32] then engages in oxidation with the amine-borane catalyst **QB5** ($E_{p/2}^{ox}$ = +1.27 V vs SCE in MeCN), either via a SET oxidation/deprotonation sequence or a concerted oxidative proton-coupled electron transfer (PCET) process, to afford the boryl radical. In turn, this nucleophilic boryl radical undergoes polarity-matched HAT with the electron-deficient C−H bond of substrates to afford electrophilic carbon radical **III**.[6a] Intermolecular addition to unactivated olefins then occurs with high levels of *anti*-Markovnikov regioselectivity to provide nucleophilic alkyl radical adduct **IV**, which is reduced by the in situ generated aryl thiol via another polarity-matched HAT event to provide the final hydroalkylation product and close the dual HAT catalytic cycle. Given the relatively low BDEs of the S−H bond of thiophenols (BDE = 80.4 kcal/mol for 2,4,6-trimethylbenzenethiol)[24] and the high BDEs of B−H bonds of amine-boranes (BDE = 100 kcal/mol for **QB5**), an alternative pathway involving HAT between the thiyl radical and the

https://doi.org/10.1021/jacs.1c05852
J. Am. Chem. Soc. 2021, 143, 11251−11261

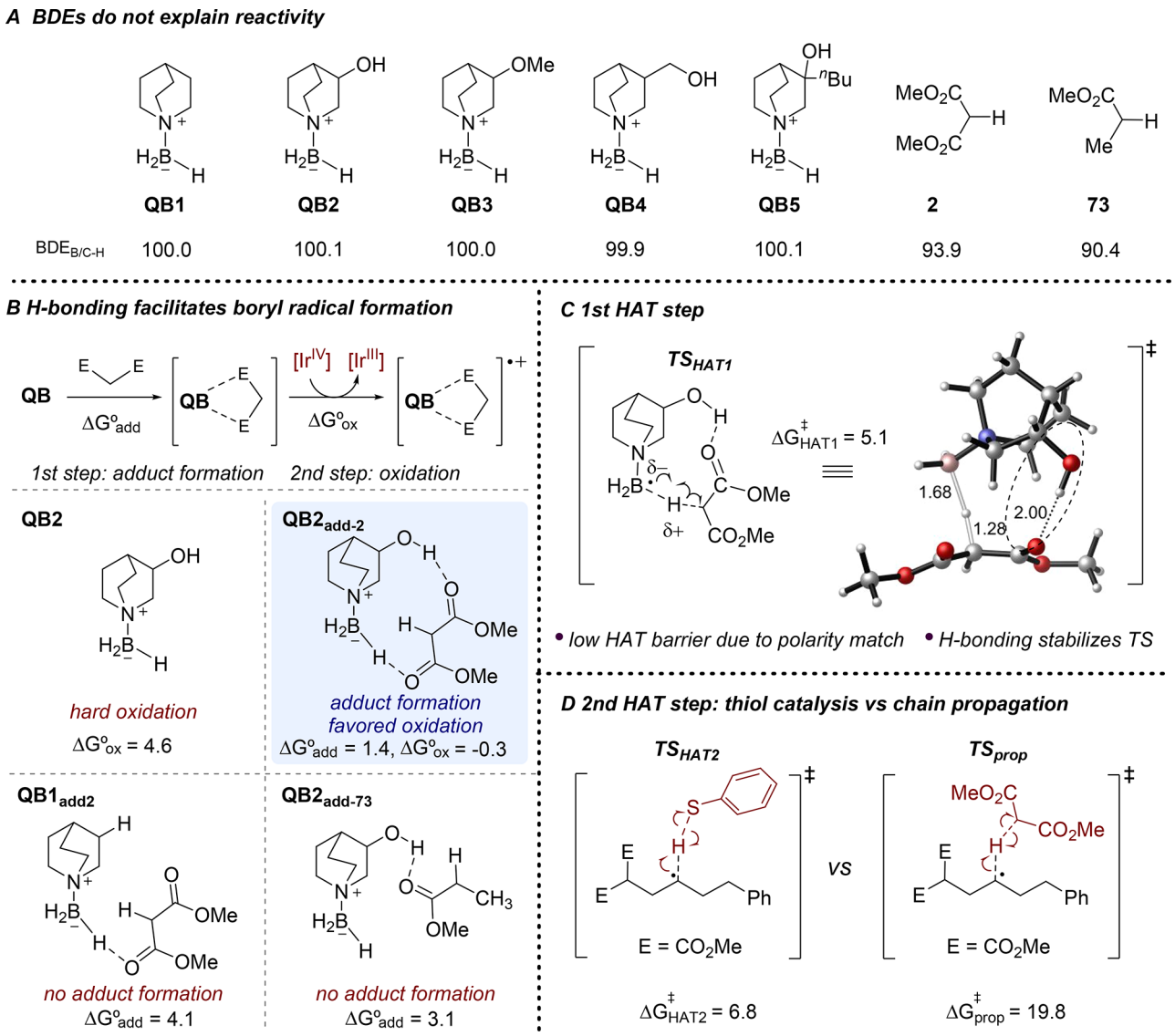

Figure 5. Density functional theory (DFT) calculations. (A) Bond dissociation energy (BDE) of the B−H bond of amine-borane catalysts and of the α-C−H bonds of selected substrates. (B) Boryl radical formation via direct oxidation of the borane catalyst or via a H-bonding assisted adduct formation/oxidation sequence. (C) HAT transition state (TS) for the formation of electrophilic carbon radical using boryl radical. (D) Transition states for the terminating HAT step using a thiol or the substrate as the H atom donor. Calculations were performed at the CPCM (benzene) M06/6-311++G(3d,2p)//M06/6-31+G(d,p) level of theory. See SI for details. All energies are given in kcal mol^{-1}. The values of the geometry information are given in Ångstroms.

amine-borane catalyst to generate the boryl radical is less favorable on thermochemical grounds. In addition, preliminary studies indicate that another pathway involving the formation of a boryl sulfide,[34] if present, is of minor importance for the observed reactivity (see SI for details).

In seeking to examine the hydrogen bonding between the amine-borane catalyst and the substrates, ^{1}H NMR titration experiments were performed and the resonance signal corresponding to the hydroxyl moiety of **QB5** was downfield shifted upon increasing concentrations of dimethyl malonate **2** (Figure 4C), indicating an O−H···O hydrogen bond might exist with the carbonyl of the malonate being the H-bond acceptor. Moreover, Job plot analysis indicates the formation of a complex between **QB5** and dimethyl malonate **2** with 1:1 stoichiometry (Figure 4D).

Computational Studies. To gain deeper insights into the mechanism of the reaction and origins of reactivity differences using different borane catalysts or substrates, we performed density functional theory (DFT) calculations at the CPCM (benzene) M06/6-311++G(3d,2p)//M06/6-31+G(d,p) level of theory (Figure 5, see SI for details). We began the calculations by calculating BDEs of the B−H bonds of the borane catalysts **QB1**−**QB5** and of the α-C−H bonds of selected substrates. It was found that bond strengths are not correlated with the catalytic efficiency shown in Table 1 as all these borane catalysts have essentially the same BDE of the B−H bond (~100 kcal/mol). In addition, the unreactive methyl propionate has a lower BDE of the α-C−H bond (90.4 kcal/mol) than that of the reactive substrate **2** (93.9 kcal/mol) (Figure 5A). We then turned to calculate the formation of the boryl radical by using **QB2** as the hydridic HAT catalyst due to its lower conformational space (Figure 5B). It was found that the borane catalyst shows a well-structured hydrogen-bonding platform that favors adduct formation with the malonate,

https://doi.org/10.1021/jacs.1c05852
J. Am. Chem. Soc. 2021, 143, 11251−11261

especially at high concentrations (ΔG°_{add} = 1.4 kcal/mol). Moreover, oxidation of this adduct to form the boryl radical is much favored as compared to the direct oxidation of the free borane catalyst (ΔG°_{ox} = 4.6 vs −0.3 kcal/mol), presumably through an oxidative PCET pathway where the carbonyl group of the malonate is acting as the base. By contrast, the absence of the hydroxyl group (**QB1**) or the H-bond acceptor (a second carbonyl group) makes the formation of the adduct much less favored, thereby decelerating the formation of the boryl radical—this is in agreement with the observed diminished reactivities. The thus formed highly nucleophilic boryl radical then undergoes a fast and polarity-matched HAT with the electron-deficient C−H bonds of the substrate (Figure 5C). This HAT step has a free energy barrier of only 5.1 kcal/mol and also exhibits the formation of H-bond in the transition state, underscoring the importance of the pendant hydroxyl group in **QB2** ($\mathbf{TS}_{HAT1}$) and allowing for fast malonyl radical formation. Finally, we explored two competitive pathways, i.e., thiol catalysis and radical chain propagation, for the terminating HAT event (Figure 5D). Interestingly, the activation barrier is significantly lowered ($\Delta\Delta G^{\ddagger}$ = 13.0 kcal/mol) by the thiol catalyst as compared to the radical chain propagation mechanism, where C−H bonds of another substrate acts as the H atom donor, in line with the measured quantum yield of the reaction.

CONCLUSION

In summary, we have developed a dual HAT protocol for the hydroalkylation of unactivated olefins with substrates containing electron-deficient C−H bonds. This approach is complementary with the well-established HAT-initiated Giese-type hydroalkylation where only hydridic or electron-neutral C−H bonds and electron-deficient olefins are amenable. This method obviates the use of prefunctionalized electrophilic carbon radical precursors and exhibits a broad scope with a high level of functional group tolerance. Experimental and computational studies reveal that hydrogen-bonding between the amine-borane catalyst and substrates is beneficial to improving the reaction efficiency. We anticipate this H-bond assisted dual HAT strategy might be extended more broadly to achieve otherwise challenging reactions in an atom-economical fashion.

ASSOCIATED CONTENT

Supporting Information

The Supporting Information is available free of charge at https://pubs.acs.org/doi/10.1021/jacs.1c05852.

Experimental procedures and product characterization data (PDF)

Accession Codes

CCDC 2080253 contains the supplementary crystallographic data of compound **54** for this paper. These data can be obtained free of charge via www.ccdc.cam.ac.uk/data_request/cif, or by emailing data_request@ccdc.cam.ac.uk, or by contacting The Cambridge Crystallographic Data Centre, 12 Union Road, Cambridge CB2 1EZ, UK; fax: +44 1223 336033.

AUTHOR INFORMATION

Corresponding Authors

Juntao Ye − *Shanghai Key Laboratory for Molecular Engineering of Chiral Drugs, Frontiers Science Center for Transformative Molecules, School of Chemistry and Chemical Engineering, Shanghai Jiao Tong University, Shanghai 200240, China;* orcid.org/0000-0001-6389-9680; Email: juntaoye@sjtu.edu.cn

Ignacio Funes-Ardoiz − *Department of Chemistry, Centro de Investigación en Síntesis Química (CISQ), Universidad de La Rioja, 26006 Logroño, Spain;* orcid.org/0000-0002-5843-9660; Email: ignacio.funesa@unirioja.es

Authors

Guangyue Lei − *Shanghai Key Laboratory for Molecular Engineering of Chiral Drugs, Frontiers Science Center for Transformative Molecules, School of Chemistry and Chemical Engineering, Shanghai Jiao Tong University, Shanghai 200240, China*

Meichen Xu − *Shanghai Key Laboratory for Molecular Engineering of Chiral Drugs, Frontiers Science Center for Transformative Molecules, School of Chemistry and Chemical Engineering, Shanghai Jiao Tong University, Shanghai 200240, China*

Rui Chang − *Shanghai Key Laboratory for Molecular Engineering of Chiral Drugs, Frontiers Science Center for Transformative Molecules, School of Chemistry and Chemical Engineering, Shanghai Jiao Tong University, Shanghai 200240, China*

Complete contact information is available at: https://pubs.acs.org/10.1021/jacs.1c05852

Author Contributions

§G.L. and M.X. contributed equally to this work.

Notes

The authors declare no competing financial interest.

ACKNOWLEDGMENTS

We dedicate this paper to the memory of Professor Ei-ichi Negishi. Financial support from the National Natural Science Foundation of China (Grant No. 22001163), "Thousand Youth Talents Plan", and Shanghai Jiao Tong University (SJTU) are acknowledged. J.Y. thanks Prof. Xianjie Fang and Prof. Gang Chen for the generous use of their analytical instrumentation and Prof. Zhaoguo Zhang for sharing laboratory space during the initial stage of this project. I.F.A. thanks the University of La Rioja for financial support and the computer cluster "Beronia" for providing computational resources. Dr. Devenderan Ramanathan and Mr. Qinglong Shi from SJTU are acknowledged for reproducing the syntheses of compounds **17**, **18**, **25**, and **53**.

REFERENCES

(1) For selected reviews, see: (a) Mayer, J. M. Understanding Hydrogen Atom Transfer: From Bond Strengths to Marcus Theory. *Acc. Chem. Res.* **2011**, *44*, 36−46. (b) Salamone, M.; Bietti, M. Tuning Reactivity and Selectivity in Hydrogen Atom Transfer from Aliphatic C−H Bonds to Alkoxyl Radicals: Role of Structural and Medium Effects. *Acc. Chem. Res.* **2015**, *48*, 2895−2903. (c) Gentry, E. C.; Knowles, R. R. Synthetic Applications of Proton-Coupled Electron Transfer. *Acc. Chem. Res.* **2016**, *49*, 1546−1556. (d) Capaldo, L.; Ravelli, D. Hydrogen Atom Transfer (HAT): A Versatile Strategy for Substrate Activation in Photocatalyzed Organic Synthesis. *Eur. J. Org. Chem.* **2017**, *2017*, 2056−2071. (e) Chu, J. C. K.; Rovis, T. Complementary Strategies for Directed C(sp^3)−H Functionalization: A Comparison of Transition-Metal-Catalyzed Activation, Hydrogen Atom Transfer, and Carbene/Nitrene Transfer. *Angew. Chem., Int. Ed.* **2018**, *57*, 62−101. (f) Stateman, L.; Nakafuku, K.; Nagib, D. Remote C−H Functionalization via Selective Hydrogen Atom Transfer.

Synthesis **2018**, *50*, 1569−1586. (g) Nakano, Y.; Biegasiewicz, K. F.; Hyster, T. K. Biocatalytic Hydrogen Atom Transfer: An Invigorating Approach to Free-Radical Reactions. *Curr. Opin. Chem. Biol.* **2019**, *49*, 16−24. (h) Liu, D.; Zhang, J.; Chen, Y. Investigations on the 1,2-Hydrogen Atom Transfer Reactivity of Alkoxyl Radicals under Visible-Light-Induced Reaction Conditions. *Synlett* **2021**, *32*, 356−361. (i) Zhang, Z.-H.; Wei, H.; Li, Z.-L.; Liu, X.-Y. Recent Advances in Radical-Involved Alkynylation of Unactivated C(sp^3)−H Bonds by Hydrogen Atom Abstraction. *Synlett* **2021**, *32*, 362−368. (j) Cao, H.; Tang, X.; Tang, H.; Yuan, Y.; Wu, J. Photoinduced Intermolecular Hydrogen Atom Transfer Reactions in Organic Synthesis. *Chem. Catal.* **2021**, DOI: 10.1016/j.checat.2021.04.008.

(2) For a special issue on "Hydrogen Atom Transfer", see: Costas, M.; Bietti, M. Uncovering the Complexity of the Simplest Atom Transfer Reaction. *Acc. Chem. Res.* **2018**, *51*, 2601−2602.

(3) *Visible Light Photocatalysis in Organic Chemistry*; Stephenson, C. R. J., Yoon, T. P., MacMillan, D. W. C., Eds.; Wiley: Weinheim, 2018.

(4) For selected recent reviews, see: (a) Skubi, K. L.; Blum, T. R.; Yoon, T. P. Dual Catalysis Strategies in Photochemical Synthesis. *Chem. Rev.* **2016**, *116*, 10035−10174. (b) Staveness, D.; Bosque, I.; Stephenson, C. R. J. Free Radical Chemistry Enabled by Visible Light-Induced Electron Transfer. *Acc. Chem. Res.* **2016**, *49*, 2295−2306. (c) Romero, N. A.; Nicewicz, D. A. Organic Photoredox Catalysis. *Chem. Rev.* **2016**, *116*, 10075−10166. (d) Twilton, J.; Le, C.; Zhang, P.; Shaw, M. H.; Evans, R. W.; MacMillan, D. W. C. The Merger of Transition Metal and Photocatalysis. *Nat. Rev. Chem.* **2017**, *1*, 0052. (e) Marzo, L.; Pagire, S. K.; Reiser, O.; König, B. Visible-Light Photocatalysis: Does It Make a Difference in Organic Synthesis? *Angew. Chem., Int. Ed.* **2018**, *57*, 10034−10072. (f) Silvi, M.; Melchiorre, P. Enhancing the Potential of Enantioselective Organocatalysis with Light. *Nature* **2018**, *554*, 41−49. (g) Strieth-Kalthoff, F.; James, M. J.; Teders, M.; Pitzer, L.; Glorius, F. Energy Transfer Catalysis Mediated by Visible Light: Principles, Applications, Directions. *Chem. Soc. Rev.* **2018**, *47*, 7190−7202. (h) Chen, Y.; Lu, L.-Q.; Yu, D.-G.; Zhu, C.-J.; Xiao, W.-J. Visible Light-Driven Organic Photochemical Synthesis in China. *Sci. China: Chem.* **2019**, *62*, 24−57. (i) Crespi, S.; Fagnoni, M. Generation of Alkyl Radicals: From the Tyranny of Tin to the Photon Democracy. *Chem. Rev.* **2020**, *120*, 9790−9833. (j) Yu, X.-Y.; Chen, J.-R.; Xiao, W.-J. Visible Light-Driven Radical-Mediated C−C Bond Cleavage/Functionalization in Organic Synthesis. *Chem. Rev.* **2021**, *121*, 506−561. (k) Wu, X.; Zhu, C. Radical-Mediated Remote Functional Group Migration. *Acc. Chem. Res.* **2020**, *53*, 1620−1636.

(5) Tedder, J. M. Which Factors Determine the Reactivity and Regioselectivity of Free Radical Substitution and Addition Reactions? *Angew. Chem., Int. Ed. Engl.* **1982**, *21*, 401−410.

(6) (a) Roberts, B. P. Polarity-Reversal Catalysis of Hydrogen-Atom Abstraction Reactions: Concepts and Applications in Organic Chemistry. *Chem. Soc. Rev.* **1999**, *28*, 25−35. (b) Parsaee, F.; Senarathna, M. C.; Kannangara, P. B.; Alexander, S. N.; Arche, P. D. E.; Welin, E. R. Radical Philicity and its Role in Selective Organic Transformations. *Nat. Rev. Chem.* **2021**, *5*, 486−499.

(7) For selected examples, see: (a) Jin, J.; MacMillan, D. W. C. Alcohols as Alkylating Agents in Heteroarene C−H Functionalization. *Nature* **2015**, *525*, 87−90. (b) Jeffrey, J. L.; Terrett, J. A.; MacMillan, D. W. C. O−H Hydrogen Bonding Promotes H-Atom Transfer from α C−H Bonds for C-Alkylation of Alcohols. *Science* **2015**, *349*, 1532−1536. (c) Mukherjee, S.; Maji, B.; Tlahuext-Aca, A.; Glorius, F. Visible Light-Promoted Activation of Unactivated C(sp^3)−H Bonds and Their Selective Trifluoromethylthiolation. *J. Am. Chem. Soc.* **2016**, *138*, 16200−16203. (d) Shields, B. J.; Doyle, A. G. Direct C(sp^3)−H Cross Coupling Enabled by Catalytic Generation of Chlorine Radicals. *J. Am. Chem. Soc.* **2016**, *138*, 12719−12722. (e) Deng, H. P.; Fan, X. Z.; Chen, Z. H.; Xu, Q. H.; Wu, J. Photoinduced Nickel-Catalyzed Chemo- and Regioselective Hydroalkylation of Internal Alkynes with Ether and Amide α-Hetero C(sp^3)−H Bonds. *J. Am. Chem. Soc.* **2017**, *139*, 13579−13584. (f) Hu, A.; Guo, J.-J.; Pan, H.; Zuo, Z. Selective Functionalization of Methane, Ethane, and Higher Alkanes by Cerium Photocatalysis. *Science* **2018**, *361*, 668−672. (g) Margrey, K. A.; Czaplyski, W. L.; Nicewicz, D. A.; Alexanian, E. J. A General Strategy for Aliphatic C−H Functionalization Enabled by Organic Photoredox Catalysis. *J. Am. Chem. Soc.* **2018**, *140*, 4213−4217. (h) Tanaka, H.; Sakai, K.; Kawamura, A.; Oisaki, K.; Kanai, M. Sulfonamides as New Hydrogen Atom Transfer (HAT) Catalysts for Photoredox Allylic and Benzylic C−H Arylations. *Chem. Commun.* **2018**, *54*, 3215−3218. (i) Wang, Y.; Carder, H. M.; Wendlandt, A. E. Synthesis of Rare Sugar Isomers Through Site-Selective Epimerization. *Nature* **2020**, *578*, 403−408. (j) Ryder, A. S. H.; Cunningham, W. B.; Ballantyne, G.; Mules, T.; Kinsella, A. G.; Turner-Dore, J.; Alder, C. M.; Edwards, L. J.; McKay, B. S. J.; Grayson, M. N.; Cresswell, A. J. Photocatalytic α-Tertiary Amine Synthesis via C−H Alkylation of Unmasked Primary Amines. *Angew. Chem., Int. Ed.* **2020**, *59*, 14986−14991. (k) Shu, C.; Noble, A.; Aggarwal, V. K. Metal-Free Photoinduced C(sp^3)−H Borylation of Alkanes. *Nature* **2020**, *586*, 714−719. (l) Ohmatsu, K.; Suzuki, R.; Furukawa, Y.; Sato, M.; Ooi, T. Zwitterionic 1,2,3-Triazolium Amidate as a Catalyst for Photoinduced Hydrogen-Atom Transfer Radical Alkylation. *ACS Catal.* **2020**, *10*, 2627−2632. (m) McMillan, A. J.; Sieńkowska, M.; Lorenzo, P. D.; Gransbury, G. K.; Chilton, N. F.; Salamone, M.; Ruffoni, A.; Bietti, M.; Leonori, D. Practical and Selective sp^3 C−H Bond Chlorination via Aminium Radicals. *Angew. Chem., Int. Ed.* **2021**, *60*, 7132−7139.

(8) For selected examples, see: (a) Xia, J.-B.; Zhu, C.; Chen, C. Visible Light-Promoted Metal-Free C−H Activation: Diarylketone-Catalyzed Selective Benzylic Mono- and Difluorination. *J. Am. Chem. Soc.* **2013**, *135*, 17494−17500. (b) Shen, Y.; Gu, Y.; Martin, R. sp^3 C−H Arylation and Alkylation Enabled by the Synergy of Triplet Excited Ketones and Nickel Catalysts. *J. Am. Chem. Soc.* **2018**, *140*, 12200−12209. (c) Li, Y.; Lei, M.; Gong, L. Photocatalytic Regio- and Stereoselective C(sp^3)−H Functionalization of Benzylic and Allylic Hydrocarbons as well as Unactivated Alkanes. *Nat. Catal.* **2019**, *2*, 1016−1026. (d) Dewanji, A.; Krach, P. E.; Rueping, M. The Dual Role of Benzophenone in Visible-Light/Nickel Photoredox-Catalyzed C-H Arylations: Hydrogen-Atom Transfer and Energy Transfer. *Angew. Chem., Int. Ed.* **2019**, *58*, 3566−3570. (e) Niu, L.; Jiang, C.; Liang, Y.; Liu, D.; Bu, F.; Shi, R.; Chen, H.; Chowdhury, A. D.; Lei, A. Manganese-Catalyzed Oxidative Azidation of C(sp^3)−H Bonds under Electrophotocatalytic Conditions. *J. Am. Chem. Soc.* **2020**, *142*, 17693−17702. (f) Lee, W.; Jung, S.; Kim, M.; Hong, S. Site-Selective Direct C−H Pyridylation of Unactivated Alkanes by Triplet Excited Anthraquinone. *J. Am. Chem. Soc.* **2021**, *143*, 3003−3012.

(9) For selected recent examples, see: (a) Murphy, J.; Bastida, D.; Paria, S.; Fagnoni, M.; Melchiorre, P. Asymmetric Catalytic Formation of Quaternary Carbons by Iminium Ion Trapping of Radicals. *Nature* **2016**, *532*, 218−222. (b) Perry, I. B.; Brewer, T. F.; Sarver, P. J.; Schultz, D. M.; DiRocco, D. A.; MacMillan, D. W. C. Direct Arylation of Strong Aliphatic C−H Bonds. *Nature* **2018**, *560*, 70−75. (c) Laudadio, G.; Deng, Y.; van der Wal, K.; Ravelli, D.; Nuño, M.; Fagnoni, M.; Guthrie, D.; Sun, Y.; Noël, T. C(sp^3)−H Functionalizations of Light Hydrocarbons Using Decatungstate Photocatalysis in Flow. *Science* **2020**, *369*, 92−96. (d) Fan, P.; Lan, Y.; Zhang, C.; Wang, C. Nickel/Photo-Cocatalyzed Asymmetric Acyl-Carbamoylation of Alkenes. *J. Am. Chem. Soc.* **2020**, *142*, 2180−2186. (e) Cao, H.; Kuang, Y.; Shi, X.; Wong, K. L.; Tan, B. B.; Kwan, J. M. C.; Liu, X.; Wu, J. Photoinduced Site-Selective Alkenylation of Alkanes and Aldehydes with Aryl Alkenes. *Nat. Commun.* **2020**, *11*, 1956. (f) Xu, S.; Chen, H.; Zhou, Z.; Kong, W. Three-Component Alkene Difunctionalization by Direct and Selective Activation of Aliphatic C−H Bonds. *Angew. Chem., Int. Ed.* **2021**, *60*, 7405−7411.

(10) For selected examples, see: (a) Fan, X.-Z.; Rong, J.-W.; Wu, H.-L.; Zhou, Q.; Deng, H.-P.; Tan, J. D.; Xue, C.-W.; Wu, L.-Z.; Tao, H.-R.; Wu, J. Eosin Y as a Direct Hydrogen-Atom Transfer Photocatalyst for the Functionalization of C−H Bonds. *Angew. Chem., Int. Ed.* **2018**, *57*, 8514−8518. (b) Kuang, Y.; Wang, K.; Shi, X.; Huang, X.; Meggers, E.; Wu, J. Asymmetric Synthesis of 1,4-Dicarbonyl Compounds from Aldehydes by Hydrogen Atom Transfer Photocatalysis and Chiral Lewis Acid Catalysis. *Angew. Chem., Int. Ed.* **2019**, *58*, 16859−16863. (c) Yan, J.; Cheo, H. W.; Teo, W. K.; Shi, X.; Wu,

H.; Idres, S. B.; Deng, L. W.; Wu, J. A Radical Smiles Rearrangement Promoted by Neutral Eosin Y as a Direct Hydrogen Atom Transfer Photocatalyst. *J. Am. Chem. Soc.* **2020**, *142*, 11357−11362. (d) Liu, H.; Xue, F.; Wang, M.; Tang, X.; Wu, J. Neutral-Eosin Y-Catalyzed Regioselective Hydroacylation of Aryl Alkenes under Visible-Light Irradiation. *Synlett* **2021**, *32*, 406−410.

(11) For selected examples, see: (a) West, J. G.; Bedell, T. A.; Sorensen, E. J. The Uranyl Cation as a Visible-Light Photocatalyst for C(sp^3)−H Fluorination. *Angew. Chem., Int. Ed.* **2016**, *55*, 8923−8927. (b) Wu, L.; Cao, X.; Chen, X.; Fang, W.; Dolg, M. Visible-Light Photocatalysis of C(sp^3)−H Fluorination by the Uranyl Ion: Mechanistic Insights. *Angew. Chem., Int. Ed.* **2018**, *57*, 11812−11816.

(12) (a) Dang, H.-S.; Roberts, B. P. Amine-Boranes As Polarity Reversal Catalysts For Radical Chain 2,3-Epoxypropanation Reactions of Esters. *Tetrahedron Lett.* **1992**, *33*, 4621−4624. (b) Dang, H.-S.; Roberts, B. P. Homolytic Reactions of Ligated Boranes. Part 17. Amine-Boranes as Polarity Reversal Catalysts for Radical Chain Reactions of Esters with Vinylic Epoxides and with Allylic *tert*-Butyl Peroxides. *J. Chem. Soc., Perkin Trans. 1* **1993**, 891−898. (c) Cai, Y.; Dang, H.-S.; Roberts, B. P. Radical-Chain Functionalisation at C−H Centres using An O-oxiranylcarbinyl O-silyl Ketene Acetal. *Tetrahedron Lett.* **2004**, *45*, 4405−4409.

(13) For selected reviews, see: (a) Giese, B. Formation of CC Bonds by Addition of Free Radicals to Alkenes. *Angew. Chem., Int. Ed. Engl.* **1983**, *22*, 753−764. (b) Yan, M.; Lo, J. C.; Edwards, J. T.; Baran, P. S. Radicals: Reactive Intermediates with Translational Potential. *J. Am. Chem. Soc.* **2016**, *138*, 12692−12714. (c) Studer, A.; Curran, D. P. Catalysis of Radical Reactions: A Radical Chemistry Perspective. *Angew. Chem., Int. Ed.* **2016**, *55*, 58−102. (d) Yi, H.; Zhang, G.; Wang, H.; Huang, Z.; Wang, J.; Singh, A. K.; Lei, A. Recent Advances in Radical C−H Activation/Radical Cross-Coupling. *Chem. Rev.* **2017**, *117*, 9016−9085. See also ref 4i.

(14) For a review, see: (a) Fischer, H.; Radom, L. Factors Controlling the Addition of Carbon-Centered Radicals to Alkenes—An Experimental and Theoretical Perspective. *Angew. Chem., Int. Ed.* **2001**, *40*, 1340−1371. For a recent polarity umpolung strategy, see: (b) Liu, J.; Wu, S.; Yu, J.; Lu, C.; Wu, Z.; Wu, X.; Xue, X.-S.; Zhu, C. Polarity Umpolung Strategy for the Radical Alkylation of Alkenes. *Angew. Chem., Int. Ed.* **2020**, *59*, 8195−8202.

(15) For an example of using superstoichiometric amount of dicumyl peroxide as a methyl radical precursor for alkene hydroalkylation, see: Li, Z.; Xiao, Y.; Liu, Z.-Q. A Radical *anti*-Markovnikov Addition of Alkyl Nitriles to Simple Alkenes via Selective sp^3 C−H Bond Functionalization. *Chem. Commun.* **2015**, *51*, 9969−9971.

(16) For selected examples, see: (a) Yu, P.; Lin, J.-S.; Li, L.; Zheng, S.-C.; Xiong, Y.-P.; Zhao, L.-J.; Tan, B.; Liu, X.-Y. Enantioselective C−H Bond Functionalization Triggered by Radical Trifluoromethylation of Unactivated Alkene. *Angew. Chem., Int. Ed.* **2014**, *53*, 11890−11894. (b) Lin, Q.-Y.; Xu, X.-H.; Zhang, K.; Qing, F.-L. Visible-Light-Induced Hydrodifluoromethylation of Alkenes with A Bromodifluoromethylphosphonium Bromide. *Angew. Chem., Int. Ed.* **2016**, *55*, 1479−1483. (c) Huang, W.; Chen, W.; Wang, G.; Li, J.; Cheng, X.; Li, G. Thiyl-Radical-Catalyzed Photoreductive Hydrodifluoroacetamidation of Alkenes with Hantzsch Ester as a Multifunctional Reagent. *ACS Catal.* **2016**, *6*, 7471−7474. (d) Wang, H.; Jui, N. T. Catalytic Defluoroalkylation of Trifluoromethylaromatics with Unactivated Alkenes. *J. Am. Chem. Soc.* **2018**, *140*, 163−166. (e) Vogt, D. B.; Seath, C. P.; Wang, H.; Jui, N. T. Selective C−F Functionalization of Unactivated Trifluoromethylarenes. *J. Am. Chem. Soc.* **2019**, *141*, 13203−13211. (f) Yu, Y.-J.; Zhang, F.-L.; Peng, T.-Y.; Wang, C.-L.; Cheng, J.; Chen, C.; Houk, K. N.; Wang, Y.-F. Sequential C−F Bond Functionalizations of Trifluoroacetamides and Acetates via Spin-Center Shifts. *Science* **2021**, *371*, 1232−1240. (g) Su, Y.-L.; Liu, G.-X.; Liu, J.-W.; Tram, L.; Qiu, H.; Doyle, M. P. Radical-Mediated Strategies for the Functionalization of Alkenes with Diazo Compounds. *J. Am. Chem. Soc.* **2020**, *142*, 13846−13855. (h) Meyer, C. F.; Hell, S. M.; Misale, A.; Trabanco, A. A.; Gouverneur, V. Hydrodifluoromethylation of Alkenes with Difluoroacetic Acid. *Angew. Chem., Int. Ed.* **2019**, *58*, 8829−8833. (i) Yang, J.; Zhu, S.; Wang, F.; Qing, F.-L.; Chu, L. Silver-Enabled General Radical Difluoromethylation Reaction with $TMSCF_2H$. *Angew. Chem., Int. Ed.* **2021**, *60*, 4300−4306.

(17) Wayner, D. D. M.; Houmam, A.; Rømming, C.; Skattebøl, L.; Barre, L.; Hammerich, O.; Søtofte, I.; Langstrom, B. Redox Properties of Free Radicals. *Acta Chem. Scand.* **1998**, *52*, 377−384.

(18) Wallentin, C. J.; Nguyen, J. D.; Finkbeiner, P.; Stephenson, C. R. Visible Light-Mediated Atom Transfer Radical Addition via Oxidative and Reductive Quenching of Photocatalysts. *J. Am. Chem. Soc.* **2012**, *134*, 8875−8884.

(19) Tang, S.; Liu, K.; Liu, C.; Lei, A. Olefinic C(sp^3)−H Functionalization Through Radical Alkenylation. *Chem. Soc. Rev.* **2015**, *44*, 1070−1082.

(20) For recent reviews, see: (a) Taniguchi, T. Boryl Radical Addition to Multiple Bonds in Organic Synthesis. *Eur. J. Org. Chem.* **2019**, *2019*, 6308−6319. (b) Jin, J.; Xia, H.; Zhang, F.; Wang, Y. Lewis-Base Boryl Radicals Enabled Borylation, Radical Catalysis and Reduction Reactions. *Youji Huaxue* **2020**, *40*, 2185−2194. (c) Tian, Y. M.; Guo, X. N.; Braunschweig, H.; Radius, U.; Marder, T. B. Photoinduced Borylation for the Synthesis of Organoboron Compounds. *Chem. Rev.* **2021**, *121*, 3561−3597.

(21) For a seminal review, see: (a) Curran, D. P.; Solovyev, A.; Makhlouf Brahmi, M.; Fensterbank, L.; Malacria, M.; Lacôte, E. Synthesis and Reactions of N-Heterocyclic Carbene Boranes. *Angew. Chem., Int. Ed.* **2011**, *50*, 10294−10317. For selected examples, see: (b) Zhou, N.-N.; Yuan, X.-A.; Zhao, Y.; Xie, J.; Zhu, C.-J. Synergistic Photoredox Catalysis and Organocatalysis for Inverse Hydroboration of Imines. *Angew. Chem., Int. Ed.* **2018**, *57*, 3990−3994. (c) Xu, W.; Jiang, H.; Leng, J.; Ong, H.-W.; Wu, J. Visible−Light−Induced Selective Defluoroborylation of Polyfluoroarenes, gem−Difluoroalkenes, and Trifluoromethylalkenes. *Angew. Chem., Int. Ed.* **2020**, *59*, 4009−4016. (d) Xia, P. J.; Song, D.; Ye, Z.-P.; Hu, Y.-Z.; Xiao, J.-A.; Xiang, H.-Y.; Chen, X.-Q.; Yang, H. Photoinduced Single-Electron-Transfer Process as An Enabling Principle in Radical Borylation of Alkenes with NHC-Borane. *Angew. Chem., Int. Ed.* **2020**, *59*, 6706−6710. (e) Dai, W.; Geib, S. J.; Curran, D. P. 1,4-Hydroboration Reactions of Electron-Poor Aromatic Rings by N-Heterocyclic Carbene Boranes. *J. Am. Chem. Soc.* **2020**, *142*, 6261−6267. (f) Qi, J.; Zhang, F.-L.; Jin, J.-K.; Zhao, Q.; Li, B.; Liu, L.-X.; Wang, Y.-F. *Angew. Chem., Int. Ed.* **2020**, *59*, 12876−12884. (g) Zhu, C.; Dong, J.; Liu, X.; Gao, L.; Zhao, Y.; Xie, J.; Li, S.; Zhu, C.-J. Photoredox Controlled *β*-Regioselective Radical Hydroboration of Activated Alkenes with NHC-Boranes. *Angew. Chem., Int. Ed.* **2020**, *59*, 12817−12821.

(22) For a review, see: (a) Dénès, F.; Pichowicz, M.; Povie, G.; Renaud, P. Thiyl Radicals in Organic Synthesis. *Chem. Rev.* **2014**, *114*, 2587−2693. For selected examples, see: (b) Tyson, E. L.; Ament, M. S.; Yoon, T. P. Transition Metal Photoredox Catalysis of Radical Thiol−Ene Reactions. *J. Org. Chem.* **2013**, *78*, 2046−2050. (c) Teders, M.; Henkel, C.; Anhäuser, L.; Strieth-Kalthoff, F.; Gómez-Suárez, A.; Kleinmans, R.; Kahnt, A.; Rentmeister, A.; Guldi, D.; Glorius, F. The Energy-Transfer-Enabled Biocompatible Disulfide−Ene Reaction. *Nat. Chem.* **2018**, *10*, 981−988.

(23) Ueng, S.-H.; Makhlouf Brahmi, M.; Derat, É.; Fensterbank, L.; Lacôte, E.; Malacria, M.; Curran, D. P. Complexes of Borane and N-Heterocyclic Carbenes: A New Class of Radical Hydrogen Atom Donor. *J. Am. Chem. Soc.* **2008**, *130*, 10082−10083.

(24) Luo, Y.-R. *Handbook of Bond Dissociation Energies in Organic Compounds*; CRC Press: Boca Raton, 2003.

(25) For recent reviews, see: (a) Lv, X.; Xu, H.; Yin, Y.; Zhao, X.; Jiang, Z. Visible Light-Driven Cooperative DPZ and Chiral Hydrogen-Bonding Catalysis. *Chin. J. Chem.* **2020**, *38*, 1480−1488. (b) Proctor, R. S. J.; Colgan, A. C.; Phipps, R. J. Exploiting Attractive Non-Covalent Interactions for the Enantioselective Catalysis of Reactions Involving Radical Intermediates. *Nat. Chem.* **2020**, *12*, 990−1004. For selected recent examples, see: (c) Roos, C. B.; Demaerel, J.; Graff, D. E.; Knowles, R. R. Enantioselective Hydroamination of Alkenes with Sulfonamides Enabled by Proton-Coupled Electron Transfer. *J. Am. Chem. Soc.* **2020**, *142*, 5974−5979.

https://doi.org/10.1021/jacs.1c05852
J. Am. Chem. Soc. 2021, 143, 11251−11261

(d) Campbell, M. W.; Yuan, M.; Polites, V. C.; Gutierrez, O.; Molander, G. A. Photochemical C−H Activation Enables Nickel-Catalyzed Olefin Dicarbofunctionalization. *J. Am. Chem. Soc.* **2021**, *143*, 3901−3910. (e) Shen, X.; Huang, C.; Yuan, X.-A.; Yu, S. Diastereoselective and Stereodivergent Synthesis of 2-Cinnamylpyrrolines Enabled by Photoredox-Catalyzed Iminoalkenylation of Alkenes. *Angew. Chem., Int. Ed.* **2021**, *60*, 9672−9679. (f) Kong, M.; Tan, Y.; Zhao, X.; Qiao, B.; Tan, C.-H.; Cao, S.; Jiang, Z. Catalytic Reductive Cross Coupling and Enantioselective Protonation of Olefins to Construct Remote Stereocenters for Azaarenes. *J. Am. Chem. Soc.* **2021**, *143*, 4024−4031.

(26) (a) Romero, N. A.; Nicewicz, D. A. Mechanistic Insight into the Photoredox Catalysis of *Anti*-Markovnikov Alkene Hydrofunctionalization Reactions. *J. Am. Chem. Soc.* **2014**, *136*, 17024−17035. (b) Qin, Y.; Zhu, Q.; Sun, R.; Ganley, J. M.; Knowles, R. R.; Nocera, D. G. Mechanistic Investigation and Optimization of Photoredox Anti-Markovnikov Hydroamination. *J. Am. Chem. Soc.* **2021**, *143*, 10232−10242.

(27) Paul, V.; Roberts, B. P. Homolytic Reactions of Ligated Boranes. Part 8. Electron Spin Resonance Studies of Radicals derived from Ligated Alkylboranes. *J. Chem. Soc., Perkin Trans. 2* **1988**, 1183−1193.

(28) For selected reviews, see: (a) Snider, B. B. Manganese(III)-Based Oxidative Free-Radical Cyclizations. *Chem. Rev.* **1996**, *96*, 339−364. (b) Mondal, M.; Bora, U. Recent Advances In Manganese(III) Acetate Mediated Organic Synthesis. *RSC Adv.* **2013**, *3*, 18716−18754. For selected examples, see: (c) Linker, T.; Sommermann, T.; Kahlenberg, F. The Addition of Malonates to Glycals: A General and Convenient Method for the Synthesis of 2-C-Branched Carbohydrates. *J. Am. Chem. Soc.* **1997**, *119*, 9377−9384. (d) Linker, T.; Kersten, B.; Linker, U.; Peters, K.; Peters, E.-M.; von Schnering, H. G. Manganese(III)-Mediated Radical Additions of Dimethyl Malonate to Olefins. The Chemoselective Synthesis of Diesters and Lactones. *Synlett* **1996**, *1996*, 468−470. (e) Hirase, K.; Iwahama, T.; Sakaguchi, S.; Ishii, Y. Catalytic Radical Addition of Carbonyl Compounds to Alkenes by Mn(II)/Co(II)/O_2−System. *J. Org. Chem.* **2002**, *67*, 970−973.

(29) Kim, J. H.; Constantin, T.; Simonetti, M.; Llaveria, J.; Sheikh, N. S.; Leonori, D. A Radical Approach for the Selective C−H Borylation of Azines. *Nature* **2021**, DOI: 10.1038/s41586-021-03637-6.

(30) For selected examples, see: (a) Ohashi, M.; Nakatani, K.; Maeda, H.; Mizuno, K. Photochemical Monoalkylation of Propanedinitrile by Electron-Rich Alkenes. *Org. Lett.* **2008**, *10*, 2741−2743. (b) Ohashi, M.; Nakatani, K.; Maeda, H.; Mizuno, K. Selective Photochemical Monoalkylation of Active Methylene Compounds by Alkenes. A Green Pathway for Carbon−Carbon Bond Formation. *J. Photochem. Photobiol., A* **2010**, *214*, 161−170. (c) Baś, S.; Yamashita, Y.; Kobayashi, S. Development of Brønsted Base−Photocatalyst Hybrid Systems for Highly Efficient C−C Bond Formation Reactions of Malonates with Styrenes. *ACS Catal.* **2020**, *10*, 10546−10550.

(31) Nguyen, S. T.; Zhu, Q.; Knowles, R. R. PCET-Enabled Olefin Hydroamidation Reactions with *N*-Alkyl Amides. *ACS Catal.* **2019**, *9*, 4502−4507.

(32) Ladouceur, S.; Fortin, D.; Zysman-Colman, E. Enhanced Luminescent Iridium(III) Complexes Bearing Aryltriazole Cyclometallated Ligands. *Inorg. Chem.* **2011**, *50*, 11514−11526.

(33) Godsk Larsen, A.; Hjarbaek Holm, A.; Roberson, M.; Daasbjerg, K. Substituent Effects on the Oxidation and Reduction Potentials of Phenylthiyl Radicals in Acetonitrile. *J. Am. Chem. Soc.* **2001**, *123*, 1723−1729.

(34) (a) Pan, X. C.; Vallet, A. L.; Schweizer, S.; Dahbi, K.; Delpech, B.; Blanchard, N.; Graff, B.; Geib, S. J.; Curran, D. P.; Lalevée, J.; Lacôte, E. Mechanistic and Preparative Studies of Radical Chain Homolytic Substitution Reactions of *N*-Heterocyclic Carbene Boranes and Disulfides. *J. Am. Chem. Soc.* **2013**, *135*, 10484−10491. (b) Telitel, S.; Vallet, A.-L.; Schweizer, S.; Delpech, B.; Blanchard, N.; Morlet-Savary, F.; Graff, B.; Curran, D. P.; Robert, M.; Lacôte, E.; Lalevée, J. Formation of *N*-Heterocyclic Carbene−Boryl Radicals through Electrochemical and Photochemical Cleavage of the B−S bond in *N*-Heterocyclic Carbene−Boryl Sulfides. *J. Am. Chem. Soc.* **2013**, *135*, 16938−16947.

https://doi.org/10.1021/jacs.1c05852
J. Am. Chem. Soc. 2021, 143, 11251−11261